Proceedings of Engineering and Technology Innovation, vol. 28, 2024, pp. 41-54

Multifeatured Electronic Helmet to Enhance Road Safety and Rider's Comfort

Vijay Mahadev Mane, Harshal Ambadas Durge*

Department of Electronic and Telecommunication Engineering, Vishwakarma Institute of Technology, Pune, India

Received 19 April 2024; received in revised form 24 September 2024; accepted 30 September 2024

DOI: https://doi.org/10.46604/peti.2024.13598

Abstract

This paper presents a multi-featured electronic helmet designed to tackle critical road safety issues, including accidents, drunk driving, and over-speeding. The design incorporates a global system for mobile communications (GSM) and global positioning system (GPS) modules to accurately capture driver's current location and send messages to predefined contacts. When encountering an accident, the helmet promptly notifies designated contacts and authorities, ensuring swift assistance. By integrating features for detecting over-speeding, accidents, and drunk driving, the helmet renders real-time alerts to both the driver's family and traffic police, enhancing accountability and safety measures. Additionally, the helmet includes solar charging functionality for mobile devices receive 100% charged in 3.37 hours, thereby optimizing usability and emergency communication. A rain detection system protects mobile devices, while an internal warming mechanism caters to adverse weather conditions, and proffers enhanced comfort by maintaining internal form temperature between 26-27 ℃ and safety, especially in cold regions or for military personnel.

Keywords: smart helmet, accident detection, road safety technology, wearable safety devices, IoT-based safety systems

1. Introduction

In recent years, the increasing occurrences of road accidents, particularly those caused by drunk driving and overspeeding, have highlighted the urgent need for innovative solutions to enhance safety measures and expedite emergency assistance [1]. Despite ongoing efforts in traffic management, the delayed reporting of accidents in reality remains a significant obstacle to timely intervention, posing a critical challenge to road safety [2]. As a result, this paper presents a novel approach to address these issues through the development of a multi-featured electronic helmet equipped with alcohol level detection and vibration mechanisms. By promptly detecting intoxication and deterring drunk driving, this helmet aims to significantly enhance road safety, thereby mitigating the continuation of lurking perils.

Recent technological advancements have spurred innovations in road safety, with multi-featured electronic helmets representing a major step toward mitigating road risks and improving rider safety. Research by Lee et al. [3] has explored the integration of advanced sensors and communication modules into helmets, proposing a comprehensive system that combines alcohol and accident detection with global positioning system (GPS) tracking for real-time alerts. However, as a limitation, their studies lacked rigorous testing across diverse conditions, signifying the need for further exploration of system reliability.

The investigation into integrating solar charging and weather detection systems in helmets is presented by Chen et al. [4], highlighting the feasibility of incorporating solar panels for charging and rain detection to protect electronics. Despite such a contribution, extensive field testing was observably absent, necessitating further validation of these features' effectiveness in

* Corresponding author. E-mail address: harshal.durge21@vit.edu

English language proofreader: Chih-Wei Chang

real-world scenarios. Similarly, Zhou et al. [5] explored internal warming mechanisms for cold weather comfort, suggesting the use of temperature-regulated heating elements in helmet linings. While their focus was primarily on thermal comfort assessments, it warrants comprehensive evaluations of the system's efficacy across various environmental conditions and user scenarios. Moreover, the use of an MQ-3 sensor and Arduino Uno for hygienic alcohol detection furnishes real-time alerts through a buzzer and LED [6]. Although this approach outperforms existing methods, a significant limitation remains, i.e., the difficulty in distinguishing between different types of alcohol with a single sensor.

The system incorporates a radio frequency (RF) transmitter/receiver to enforce helmet use, along with an alcohol sensor featuring a red-light indicator for detecting intoxication. While these enhancements improve safety and accident prevention, potential limitations include RF interference and a restricted alcohol detection range [7]. Furthermore, a smartphone-based accident detection system utilizes accelerometers and acoustic data to notify emergency services and provide situational awareness through photos, GPS, and voice over internet protocol (VOIP), conducing in improved response times and reduced false positives [8], whereas it faces challenges related to universal availability and integration reliability.

Integrative studies assessing the synergistic effects of combined functionalities are essential for comprehensively understanding their impact on road safety. Besides, there is a paucity of research on user acceptance, usability, and regulatory compliance, which hinders the widespread adoption of advanced helmet technologies. In light of this hindrance, future research should prioritize user-centric design principles and regulatory compliance to ensure the seamless integration of advanced safety features into mainstream helmet designs. A comprehensive review of existing literature reveals a gap in research regarding proactive safety measures that effectively mitigate the risks associated with drunk driving and overspeeding. While several studies have explored the integration of GPS and global systems for mobile communication (GSM) technologies for vehicle tracking and emergency response systems, scarce research focuses specifically on incorporating these technologies into protective gear such as helmets.

This paper aims to prioritize user-centric design principles and regulatory compliance, ensuring the effective integration of advanced safety features into mainstream helmet designs. The primary objective of this study is to design and evaluate a multi-featured electronic helmet that enhances road safety by addressing critical issues such as accidents, drunk driving, and overspeeding. By leveraging GSM and GPS modules, the helmet seeks to offer real-time alerts to designated contacts and authorities in the event of an accident, facilitating prompt assistance and intervention.

2. System Connection Diagram and Features

Wontedly, the helmet system consists of three main subsystems, as sequentially mentioned as follows. The first subsystem is a notification mechanism for alcohol level, speed, and accident detection. Subsequently, the second subsystem is an internal warming system for rider comfort. Finally, the third subsystem is solar mobile charging capabilities. Key components include the pancake vibration module, electret microphone, 8 Ohm speaker, GPS Neo-6M module, GSM SIM800L module, ADXL335 sensor, LM2596 voltage regulator, and MQ-3 gas sensor, all interfaced with an Arduino Uno for notifications. A digital thermostat controls a 12V DC LED strip for internal warming. The solar mobile charging subsystem uses a 6V 1A solar panel, with additional electrical components to step down the voltage to 5V for efficient charging. A raindrop sensor, along with a buzzer interfaced with a node microcontroller unit (MCU), provides wet alerts.

2.1. System for accident, alcohol consumption level, and overspeed detection

This subsystem is responsible for detecting accidents, monitoring alcohol consumption by the rider, and measuring the speed of the motorcycle. This section outlines the design and implementation details of the subsystem. The system diagram, shown in Fig. 1, illustrates the components and connections for alcohol level, speed, and accident detection, which entails

interfacing various modules with an Arduino Uno microcontroller. The modules include the pancake vibration module, electret microphone, 8 Ohm speaker, GPS Neo-6M module, GSM SIM800L module, ADXL335 sensor, LM2596 voltage regulator, and MQ-3 gas sensor module.

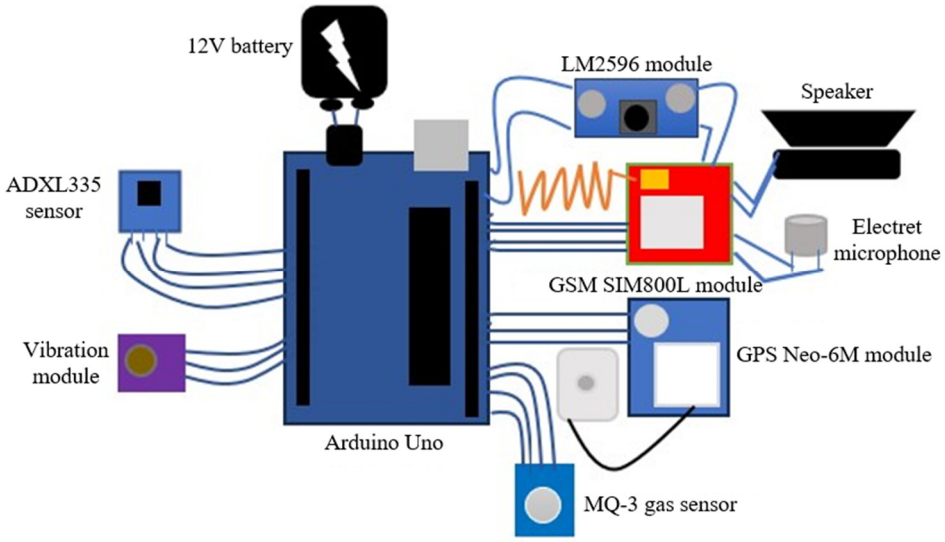

Fig. 1 GPS and GSM system for messages and calls

For alcohol consumption detection, the MQ-3 gas sensor is employed. This sensor operates based on changes in the resistance of its sensing material, known as a chemiresistor, and can detect alcohol concentrations ranging from 25 to 500 ppm. The sensor's heating system includes a nickel-chromium coil and an aluminum oxide-based ceramic coated with tin dioxide, which generates heat. To enhance safety, the sensor is enclosed within two layers of fine stainless-steel mesh, creating an "anti-explosion network". The sensing system utilizes platinum wires coated with tin dioxide to detect subtle changes in current flow across the sensing element. The sensor is comprised of six connecting legs extending from a Bakelite base. Among these six connecting legs, two legs are designated for heating the sensing element, while the remaining four legs carry signals (designated as A and B) connected to the platinum wires, as illustrated in Fig. 2.

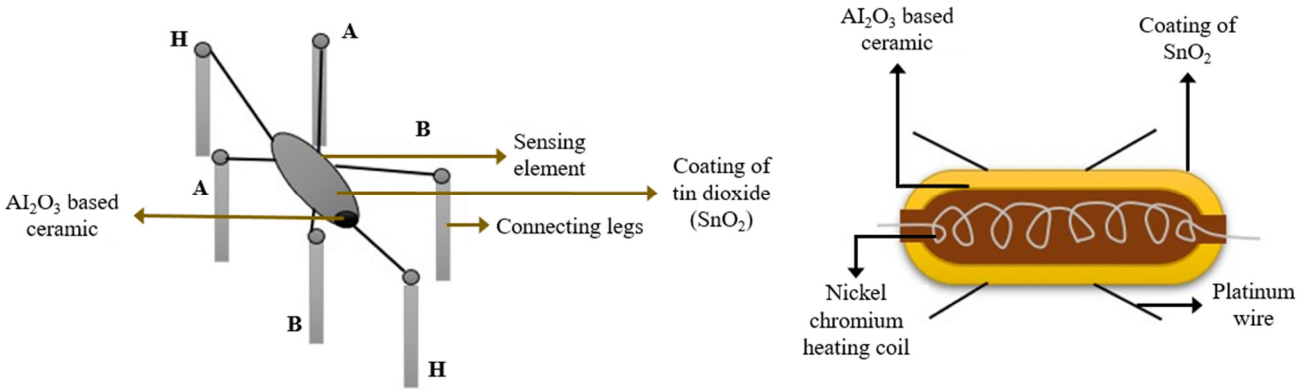

Fig. 2 Internal structure of MQ-3 gas sensor

At elevated temperatures, the SnO_2 semiconductor layer on the sensing element's surface undergoes oxygen adsorption. In clean air, electrons from the conduction band of tin dioxide are attracted to oxygen molecules, forming an electron depletion layer beneath the surface and resulting in high resistance. However, in the presence of alcohol, surface oxygen adsorption decreases as it reacts with the alcohol, reducing the potential barrier and enabling electrons to flow smoothly through the sensor.

The LM393 high-precision comparator digitizes the analog signal and transmits the data to the microcontroller, enabling the detection of alcohol levels in riders. When alcohol is detected, the system activates a vibration module to induce discomfort as a response. Predefined parameters in the microcontroller trigger commands to activate the pancake vibration modules, Neo-6M GPS, and SIM800L GSM module. Alcohol detection triggers a vibrational response as a preventive measure against drunk riding.

The pancake vibration module utilizes a piezoelectric crystal and a seismic mass to produce vibrations, which are powered by a 5V supply. These motors employ eccentric rotating mass (ERM) technology, featuring a flat printed circuit board (PCB) with a 3-pole commutation circuit around a central shaft, as shown in Fig. 3(a) and Fig. 3(b). Additionally, Fig. 3(c) illustrates the opposite surface of the commutation circuitry, which contains the voice coil assembly and counterweight.

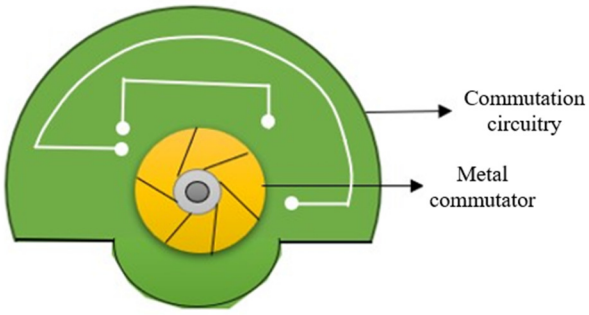

(a) Functional layer(back-side)

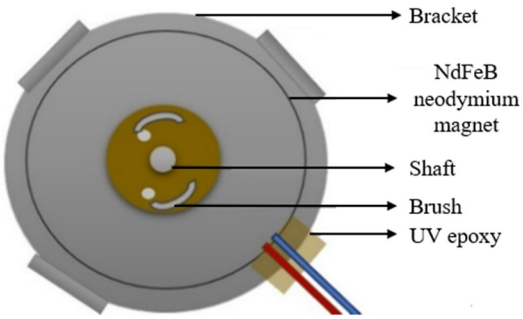

(b) Base-layer

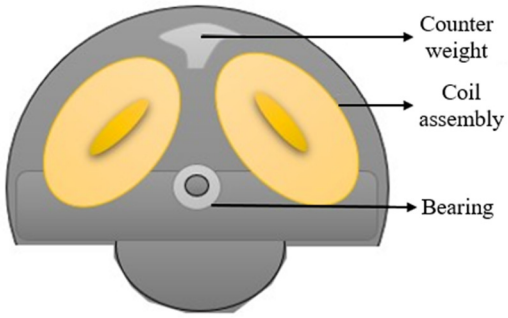

(c) Functional layer(frontside)

Fig. 3 Pancake vibration module

The power is supplied to the voice coils through brushes, creating a magnetic field that interacts with a disc magnet, generating flux. The commutation circuit reverses the magnetic field, engaging with the North-South pole pairs in the neodymium magnet. Rotation occurs due to the off-centered eccentric mass, resulting in motor vibration. The commutator configures the motor as a six-pole machine, varying resistance through the brushes during rotation. The compact design of ERM motors greatly facilitates their integration into the helmet. With a small form factor available in both cylindrical and coin-shaped designs, these motors can be easily embedded within the limited space of a helmet without adding significant weight or bulk. In the event of an accident, the ADXL335 sensor detects tilt and sends messages to the police and designated family members using a miniature cellular module that enables general packet radio service (GPRS) transmission, empowering further actions of SMS and voice calls.

The ADXL335 sensor employs a polysilicon surface-micromachined structure with signal conditioning for open-loop acceleration measurement. Polysilicon springs act as suspension elements, resisting acceleration-induced forces. Acceleration-induced deflection is measured using a differential capacitor setup, which detects the displacement of the movable mass. Phase-sensitive demodulation techniques determine both the magnitude and direction of acceleration, along with signal amplification and off-chip routing. A bandwidth-regulating capacitor enhances resolution and mitigates aliasing effects. Capacitive sensing measures microstructure displacement, providing an analog voltage output proportional to acceleration along the X, Y, and Z axes. A microcontroller converts the analog voltage to digital signals via an analog-to-digital converter (ADC) for tilt, vibration, and shock detection. Raw readings are converted into total acceleration, as shown in:

$$Total_{ACC} = \sqrt{\left(\frac{x_{axis} - 512}{256}\right)^2 + \left(\frac{y_{axis} - 512}{256}\right)^2 + \left(\frac{z_{axis} - 512}{256}\right)^2} \quad (1)$$

Upon predefined conditions, the sensor activates GPS and GSM modules to transmit the current location to designated recipients [9]. Technically, the GPS utilizes a constellation of 24 satellites orbiting the Earth to determine precise geographical coordinates. Ground (GND)-based receivers receive microwave signals from these satellites, interpreting them to calculate location, velocity, heading, and time. The Neo-6M GPS module, integrated into the system, receives raw GPS data and establishes serial communication using the Software Serial protocol. The received data is formatted in National Marine Electronics Association (NMEA) sentences, identified by a dollar sign "$" followed by specific identifiers like "GPGGA", containing vital GPS information such as 3D location and accuracy data. To extract and utilize this data effectively, character sequences within NMEA sentences are parsed and stored in variables using a designated Arduino IDE library. This library facilitates the extraction of location-related information, such as latitude and longitude, through specialized GPS functions, enhancing the usability of GPS data in various applications [10].

2.2. System for solar mobile charging

Within this subsystem, the solar mobile charging system is integrated, featuring a 6V, 1A solar panel linked to circuit box "A". Inside this box, electrical components are arranged to lower the voltage to 5V, ensuring secure mobile charging through a USB cable, as illustrated in Fig. 4(a). In addition, the system incorporates a wet alert mechanism utilizing a raindrop sensor and buzzer interfaced with node MCU, as shown in Fig. 4(b). The charging system includes key components such as a solar panel, 100 and 150-Ohm resistors, a 1N5819 diode, an LM317 voltage regulator, a BC547 NPN transistor, a 5.6V 1N4734A Zener diode, a 10K potentiometer, and a micro-USB cable. The solar panel generates the required voltage of 6V and a current of 1A.

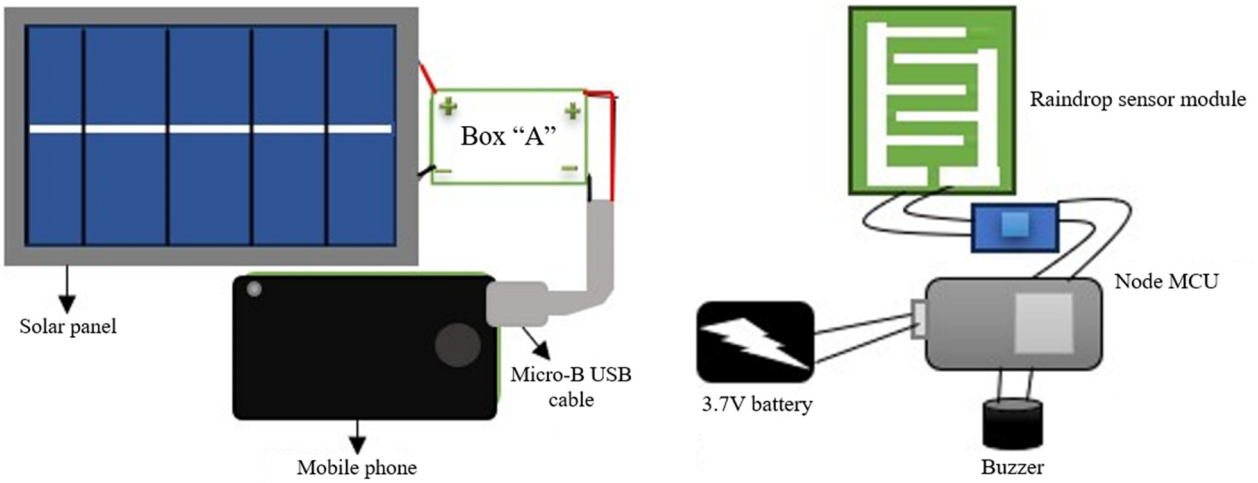

(a) Solar Module to Mobile Device Connection (b) Raindrop Sensor and Buzzer Connection with Node MCU

Fig. 4 Mobile charging and wet detection system

In solar cells, silicon atoms are arranged in a lattice structure, forming strong covalent bonds with neighboring silicon atoms. These robust bonds typically confine electrons, leading to minimal current flow. Solar cells consist of two semiconductor layers: the upper layer is doped with phosphorous to create an n-type semiconductor, while the lower layer is doped with boron to generate a p-type semiconductor. To discuss further, in the n-type layer, there is an excess of electrons, whereas the p-type layer contains surplus holes. Upon light absorption, photons with sufficient energy dislodge electrons from their bonds, causing them to migrate towards the n-side and leaving behind holes that move towards the p-side.

These electrons are collected by a thin metal layer situated at the top of the solar cell. External circuitry connects to these metal layers, enabling electrons to flow into the circuit and eventually reach a conductive aluminum sheet located at the rear of the solar cell. The electrons subsequently recombine with holes present in the p-type layer, completing the electron flow cycle within the solar cell, as shown in Fig. 5 [11]. In Fig. 4(a), the connection of the solar panel with the circuit box is depicted,

where the panel generates an output of 6V with a maximum current of 1A. The LM317 voltage regulator allows the voltage to vary up to 37V with a maximum current of 1.5A [12]. Charging mobile devices, a micro-B USB cable is utilized, featuring four pins—two designated for power transfer and the remaining two for data transfer [13].

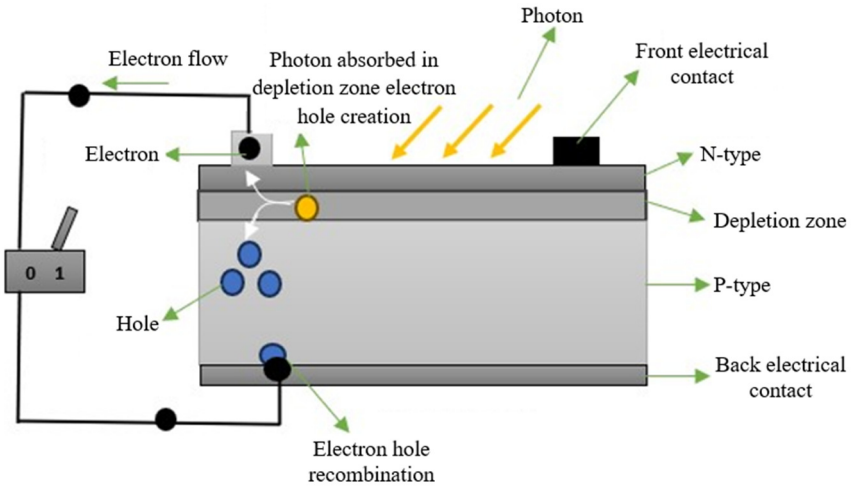

Fig. 5 Solar cell working

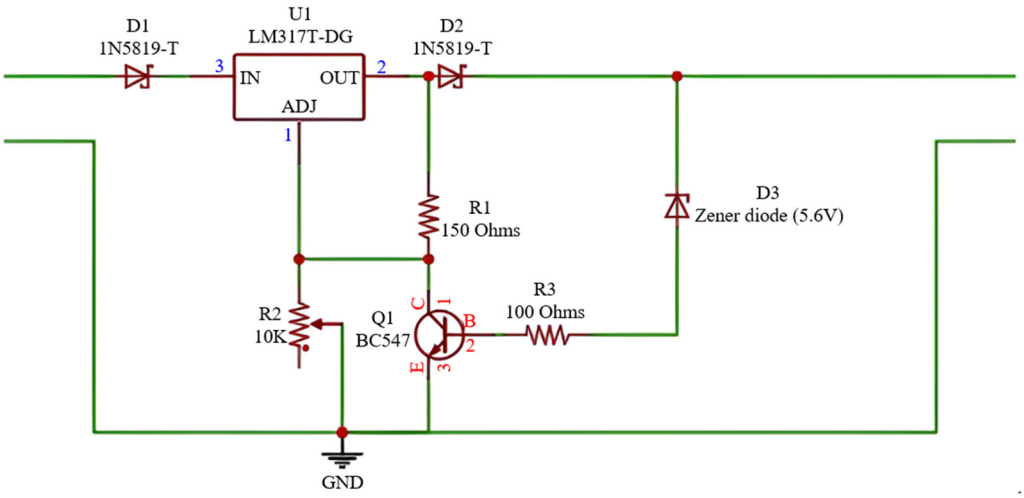

Fig. 6 Circuit of box "A"

The circuit diagram depicted in Fig. 6 includes provisions for both voltage and current regulation, alongside an over-voltage protection mechanism to ensure safe and efficient charging of mobile devices. The purpose and function of each component used in the circuit is presented as follows:

(1) Diode D1: Prevents reverse current flow from the LM317 voltage regulator back into the solar panel. This protects the solar panel from potential damage that presumably occurs if the current were to flow in the wrong direction.

(2) LM317 voltage regulator: Provides a stable and adjustable output voltage to the circuit. It takes the input voltage from the solar panel and regulates it to a desired level, which can be adjusted using the potentiometer.

(3) Diode D2: Prevents reverse voltage from damaging the circuit with the inaccessibility of any reverse current that might flow back into the LM317 voltage regulator from the output side.

(4) Zener diode: Protects the circuit from over-voltage conditions. In other words, when the voltage exceeds a certain threshold (the breakdown voltage of the Zener diode), it conducts and allows excess voltage to be safely shunted away, preventing damage to other components [14].

(5) BC547 transistor: Acts as a switch or current controller. When the Zener diode conducts due to over-voltage, the base of the BC547 transistor is activated, causing it to conduct and provide a path to the GND. This reduces the output voltage by shunting excess current, protecting the load from over-voltage.

(6) 100 Ohm resistor: Limits the base current flowing into the BC547 transistor. This ensures that the transistor operates within safe limits and is rarely susceptible to damage due to excessive current.
(7) 150 Ohm resistor: Limits the current flowing from the output of the LM317 through the BC547 transistor when it is conducting. This helps in controlling the amount of current diverted to the GND.
(8) Potentiometer: Allows for fine-tuning of the output voltage from the LM317 regulator. By adjusting the resistance, can set the desired output voltage level, conducing to the circuit rendering versatile for different applications.
(9) Micro USB cable: Provides a connection to the load. The voltage common collector (VCC) and GND wires of the cable are connected to the regulated voltage and GND, respectively, allowing the circuit to deliver a stable power supply to a connected device.

In this setup, the anode terminal of diode D1 is linked to the positive terminal of the solar panel, while the cathode terminal of diode D2 is connected to the input pin of the LM317 voltage regulator. The output terminal of the LM317 voltage regulator is linked to the anode terminal of diode D2, with the cathode terminal of D2 connected to the cathode terminal of the Zener diode. The anode terminal of the Zener diode is thereupon connected to the base of the BC547 transistor via a 100 Ohm resistor. The collector terminal of the BC547 transistor connects to the output pin of the LM317 through a 150 Ohm resistor, while the emitter terminal is GND. The adjustment pin of the LM317 is connected to the variable end of the potentiometer, which allows for voltage adjustments, and the collector terminal of the BC547. One fixed end of the potentiometer is linked to GND. Concerning the micro-USB connection, the wire connected to the VCC pin is linked to the cathode terminal of the Zener diode, and the wire connected to the GND pin of the USB cable is also GND [15].

Furthermore, the system incorporates a wet detection mechanism to alert users in the event of rain or wet conditions. This subsystem typically includes a raindrop sensor interfaced with the node MCU, which can activate an alert system to inform the rider of adverse weather conditions, enhancing safety and functionality. The rain detection system includes a raindrop sensor, node-MCU, and a buzzer to protect mobile devices while charging. The sensor operates on resistance principles: high resistance indicates dry conditions and low resistance occurs when water bridges the nickel lines on the sensor board.

This change in resistance alters the output voltage at the analog pin, which is thereafter digitized by the LM393 comparator to provide transistor-transistor logic (TTL) digital output. A potentiometer is used to adjust the comparator's threshold voltage, allowing for precise calibration. The comparator compares the threshold voltage with the analog input; if the output is high, it indicates water presence and activates the buzzer to alert the rider. Conversely, a low output signifies dry conditions. This setup ensures effective rain detection and prompt audible alerts for the rider, preventing potential water damage to the mobile device during charging [16].

2.3. System for internal warmth feature

The temperature regulation system within the helmet comprises a thermostat, an LED strip, and a power supply. Moreover, it utilizes an IP67 Waterproof Dim-to-Warm LED Light Strip, which adjusts both light intensity and color temperature to maintain optimal thermal conditions. The XH-W3001 temperature controller, known for its precision, features programmable capabilities and a relay mechanism that manages the power supply to external devices. It operates by monitoring the current temperature through an integrated negative temperature coefficient (NTC)-type thermistor, activating or deactivating the connected load as needed.

Calibration of the XH-W3001 is essential to mitigate inaccuracies that may arise from temperature probe miscalibration. This is accomplished through the temperature offset feature, allowing users to adjust displayed temperature readings to align with actual measurements. By comparing the displayed temperature with that from a calibrated sensor, the rider can determine and adjust the temperature offsets via the controller's interface. This ensures precise temperature regulation within the desired range, enhancing the system's effectiveness and functionality [17-18].

3. Features of the Helmet

The functionalities of the helmet are dichotomized into internal and external features. External features encompass capabilities such as call reception, notification alerts, and solar-powered mobile charging. Meanwhile, internal features focus on functionalities integrated within the helmet, such as internal warming systems.

3.1. External feature of the helmet

This section is divided into two parts: GPS & GSM modules for calls and alerts and solar-powered mobile charging. The first part explains the communication and alerting capabilities enabled by GPS and GSM technologies, while the second part focuses on the functionality of a solar-powered system for mobile charging.

3.1.1. GPS & GSM modules make calls and alert notification

This system integrates GPS Neo-6M and GSM Sim800l modules to address safety concerns pertinent to drunk driving, overseeding, and accidents. The GPS Neo-6M module utilizes signals from orbiting satellites to determine the helmet's current location, yielding longitude and latitude coordinates [19]. In the event of an accident or when overspeeding is detected, the system sends the rider's location to predetermined mobile numbers, including family members and the Traffic Police Control Room. To visualize the entire process, the overall workflow is shown in Fig. 7.

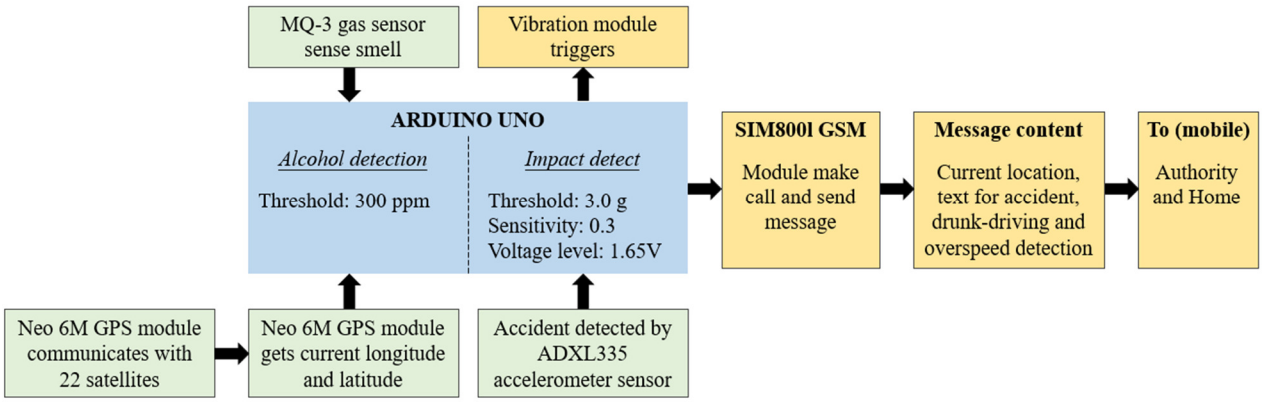

Fig. 7 Call & notification system workflow

During an accident, the ADXL335 accelerometer sensor detects changes in tilt, vibration, and rotation, triggering the system. Messages containing the rider's location are subsequently sent to the designated mobile numbers, empowering prompt responses from family members and authorities to assist [20]. The GPS module also aids in overspeed detection by continuously monitoring the rider's speed. If the speed exceeds the preset limit, notifications are sent to mobile numbers and the system generates vibrations. A call is also made to alert the traffic police, who can intervene and caution the rider about speed limits. Furthermore, if any intentionally abusive response or disregard for the ongoing call is detected, authorities can track the rider's location for further action [21]. To mitigate the risk of drunk driving, the system incorporates an MQ-3 gas sensor to detect alcohol levels. Upon detecting the level of intoxication, the helmet adjusts the intensity of vibration to alert the rider to refrain from riding [22].

Table 1 summarizes the system's performance across four key features: accident detection, alcohol detection, overspeed detection, and rain/moisture detection. Each feature is evaluated based on established safety thresholds. According to protocols set by the Department of Traffic Enforcement in India, a maximum speed limit of 50 km/h for motorcycles and a blood alcohol concentration (BAC) limit of 30 mg per 100 mL of blood (0.03% or 300 ppm) are recommended by the authorities, both of which are set as system thresholds. The wetness detection feature activates an audible alert when moisture levels fall below an ADC value of 900, protecting mobile devices from potential water damage. The accident detection system triggers a message and call system when the acceleration exceeds a threshold of 3g, as recommended by experts.

- **Accident detection**: The system successfully triggered alerts (message and call) when the g-force exceeded the 3g threshold, which aligns with real-world impacts that are considered dangerous.
- **Alcohol detection**: The microcontroller activated the vibration module when alcohol concentration exceeded predefined limits, offering effective drunk driving alerts based on traffic safety standards.
- **Overspeed detection**: The system accurately detected speeds above the 50 km/h threshold and activated warnings, ensuring that the helmet responds appropriately to speeding events.
- **Moisture detection**: Wetness was detected and alerts were triggered when moisture levels dropped below the ADC value of 900, protecting sensitive electronics from water exposure.

These thresholds were validated through simulations and testing to ensure optimal helmet performance across different conditions. The results presented in Table 1 demonstrate the system's ability to function reliably under various conditions, supporting the claims of enhanced road safety and rider protection.

Table 1 Results obtained while testing and system status recorded

Sensor	Observed value	Output	System
Accident detection (in g) (Threshold=3)			Message, call
ADXL335 Accelerometer sensor	x, y, z: 900, 850, 950 Total acc.: (2.64)	No	OFF
	1000, 900, 1000 (3.09)	Yes	ON
	1100, 1000, 1100 (3.76)	Yes	ON
	950, 950, 900 (2.85)	No	OFF
	540, 550, 520 (0.187)	No	OFF
Alcohol detection (in ppm) Range [50 >= (No), 50 < and < 300 (limited), 300 <= and 400 > (moderate), >= 400 (high)]			Message, call & vibration
MQ-3 gas sensor	41.5	No	OFF
	23.45	No	OFF
	23.5	No	OFF
	314	Yes	ON
	487	Yes	ON
Overspeed detection (in km/h) (Threshold = 50)			Vibration, message, and call
Neo-6M GPS module	51	Yes	ON
	65	Yes	ON
	44	No	OFF
	37	No	OFF
	41	No	OFF
Rain/Moisture detection (ADC value) (Threshold = 900)			Buzzer alert
Raindrop sensor	576	Yes	ON
	950	No	OFF
	801	Yes	ON
	350	Yes	ON
	455	Yes	ON

3.1.2. Solar mobile charging feature

The solar mobile charging feature allows mobile phones to be charged directly using solar panels during daylight hours. Given these devices are lightweight and portable, users can charge their phones anywhere without relying on electrical outlets. Furthermore, concerning mobile phones per se, by utilizing solar energy, mobile phones can be charged effortlessly whenever exposed to sunlight. The system is housed in a plastic box with foam padding to securely hold the mobile phone, while the solar panel is positioned on the exterior to maximize sunlight exposure. To protect the phone from water damage, a raindrop sensor triggers a buzzer alarm when water droplets are detected, prompting the user to disconnect and remove the device from

the case. Additionally, the circuit prevents battery overcharging. When the output voltage is set to 5V by adjusting the potentiometer and selecting a Zener diode with a Zener voltage (V_z) of 5V, the circuit ensures proper operation as long as the battery voltage at the charging terminal remains at or below 5V.

In case the voltage at the charging terminal exceeds 5V, the Zener diode enters reverse bias mode and begins conducting due to its Zener voltage. This, in turn, causes the BC547 transistor to operate in forward bias mode, effectively disconnecting resistor R2 from the circuit. As a result, the output voltage drops to approximately 1.25V, calculated using the LM317 formula ($V_{out} = 1.25[1 + (R2/R1)]$). Since this voltage is insufficient to charge the battery, the circuit halts further charging. The output voltage can be adjusted by changing the value of resistor R2; however, in this setup, R2 is set to zero. This mechanism ensures that the battery is protected from overcharging once it reaches the desired voltage level [23-24].

The Oppo A3S model was deployed for testing the solar mobile charger. This model is equipped with a BLP673 Lithium-ion polymer battery rated at 3.85V, with a charge limit voltage of 4.4VDC and a capacity of 4100 mAh. The solar panel used in the test produces 6V at 1A, providing 6 watts of input power. The output voltage is 5.5V with a current of 1A, delivering 5.5 watts of power through the USB port. Depth of discharge (DoD) measures the percentage of a battery's capacity that has been depleted, with higher DoD values indicating more energy consumption. By default, the DoD is set to 100% for Lithium-ion batteries and 50% for lead-acid batteries. Several steps were followed to calculate the time required for charging, as enumerated in the following statements.

(1) First, the battery capacity in watt-hours is calculated by multiplying the battery voltage (3.85V) by the battery capacity in ampere-hours (4.1 Ah), yielding 15.785 watt-hours.
(2) Next, the discharged battery capacity is determined by multiplying the battery watt-hours by the battery DoD (100%), resulting in 15.785 watt-hours.
(3) To estimate the energy required for a full battery charge, the discharged battery capacity is divided by the battery rule of thumb charge efficiency factor (99% for lithium batteries), thereby yielding 15.94 watt-hours.
(4) The solar output is adjusted to account for system losses by multiplying it by 100% minus a fixed percentage (14.08%, as per the National Renewable Energy Laboratory's PVWatts Calculator), leading to an adjusted solar output of 4.7256W.
(5) Finally, the estimated charge time is calculated by dividing the energy required for a full charge (15.94 watt-hours) by the adjusted solar output (4.7256W), resulting in a charge time of 3.3731 hours.

Thus, the total time required to charge the OPPO A3s mobile phone is approximately 3 hours and 22 minutes.

3.2. Internal feature of the helmet

The internal feature of the helmet integrates an internal heating system to enhance the rider's comfort by warming the inside of the helmet. The heating mechanism uses a double layer of cotton and foam in the helmet lining for effective heat retention. To achieve a relatively appropriate temperature, temperature regulation is controlled by an XH-W3001 12V DC thermostat, which is equipped with a built-in relay. Powered by a 12V DC source, the thermostat controls a 12V DC LED strip based on preset conditions. It monitors the current temperature using a 10k NTC thermistor sensor, compares it to the predefined temperature settings, and adjusts the relay state accordingly [25].

The LED strip serves as the heat source, converting electrical energy into heat to warm the foam. The system is configured with start and stop temperatures set at 26 ℃and 27 ℃, respectively, as recommended by medical science experts to maintain an optimal foam temperature. The operational flow is illustrated in Fig. 8. When the ambient temperature falls below 26 ℃, the thermostat activates the relay, causing the LED strip to generate heat and raise the foam's temperature. As the temperature approaches approximately 27 ℃, the relay disengages, allowing the temperature to drop. This cycle continues until the power is interrupted. Graphical representations show the thermostat's ability to modulate the LED activation in response to ambient temperature changes, ensuring that the foam temperature stays within the desired 26-27 ℃ range.

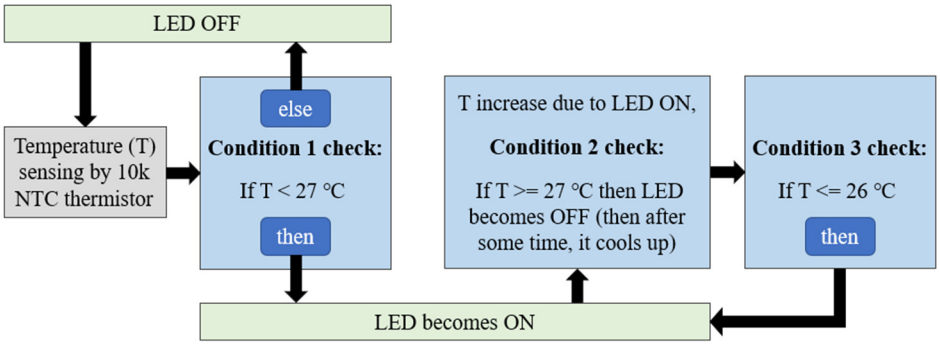

Fig. 8 Working flow of warming feature

Fig. 9 illustrates the temperature regulation graph obtained during the testing on the serial plotter of Arduino IDE, and the graph illustrates the reading of the temperature in degrees Celsius versus time in seconds, with the total observation duration being 500 seconds. Initially, the detected temperature was 26.4 °C, which is below the maximum threshold of 27 °C. Thus, the LED strip generated warmth, causing the temperature to rise. Upon reaching the maximum threshold, the LED strip is deactivated. The warmth was maintained for 220 seconds. Afterward, a subsequent temperature decrease was observed, with the graph showing a decline until it reached the minimum threshold of 26 °C, at which point the LED was reactivated. Despite this, the temperature continued to drop to 25.7 °Cbefore rising again due to the sustained external cooling. This cyclical process continued. This ensures optimal comfort for the rider by maintaining a consistent and comfortable temperature level inside the helmet.

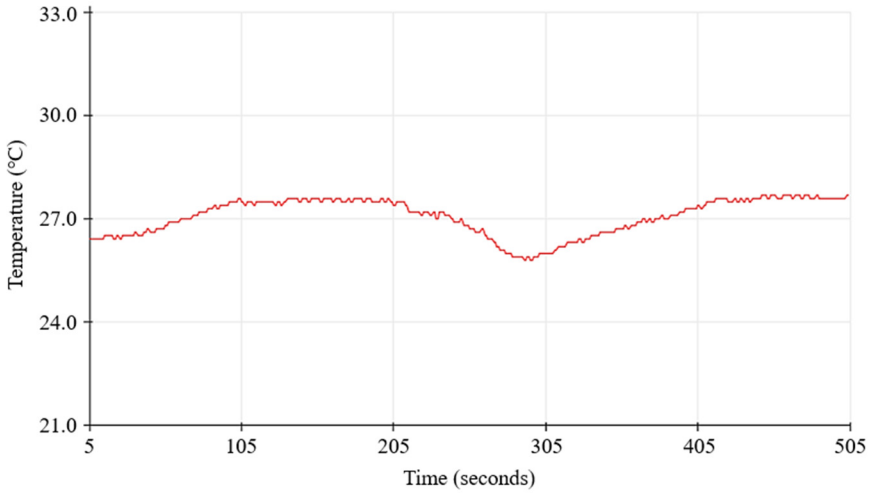

Fig. 9 Graph of internal warmth feature

4. System's Position on the Helmet

Fig. 10 illustrates the arrangement of the module, and Fig. 10(a) denotes the schematic layout of the thermostat, LED strip, and NTC thermistor positioned inside the helmet. Fig. 10(b) indicates the positioning of the solar panel and wet detection system at the backside of the helmet. Fig. 10(c) delineates the placement of vibration modules and MQ-3 gas sensors to ensure optimal spatial allocation for odor detection. The multi-featured electronic helmet was evaluated through a series of tests to assess its effectiveness in addressing critical road safety issues. The accident detection system, equipped with the ADXL335 accelerometer, ideally triggered notifications when impacts exceeded the 3g threshold, demonstrating accurate response to potential accidents. The MQ-3 gas sensor reliably detected alcohol concentrations, rendering alerts when levels reached 300 ppm, ensuring proper drunk driving detection.

Regarding overspeed detection, the Neo-6M GPS module activated alerts for speeds over 50 km/h, confirming the system's reliability in monitoring vehicle speed. The helmet's raindrop sensor accurately detected moisture levels, triggering alerts when necessary. Additionally, solar charging capabilities and an internal warming system ensured the continuous

operation of mobile devices and regulated temperature effectively. The results confirm that the helmet effectively integrates its advanced features, providing reliable alerts for accident detection, drunk driving, and over-speeding, while also offering practical solutions for solar charging, rain detection, and temperature regulation. These findings support the helmet's potential to significantly enhance road safety and user comfort.

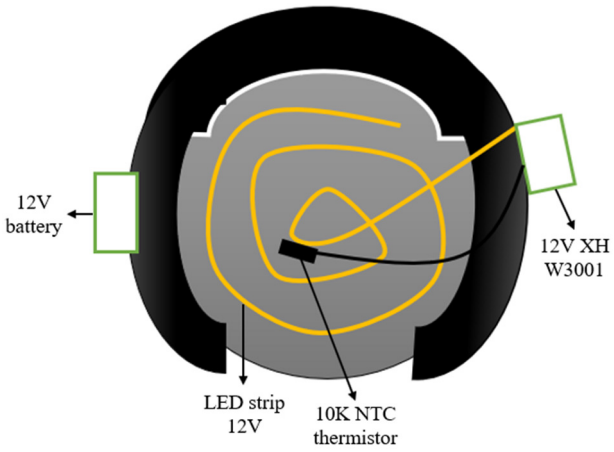

(a) Internal warmth setup

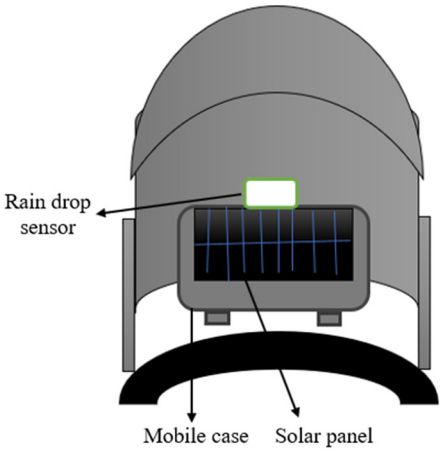

(b) Charging and rain detection setup

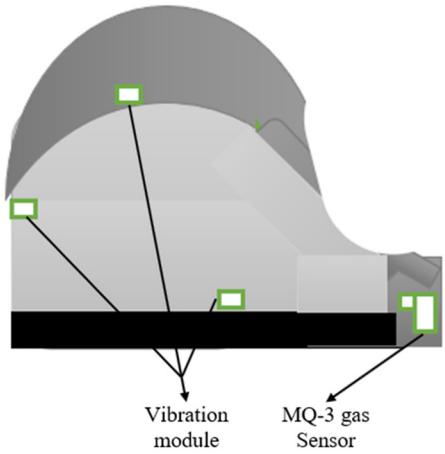

(c) Alcohol detection and vibrational response setup

Fig. 10 Placement of warming, alcohol detection, charging, and wet detection system on the helmet

5. Conclusion

This paper presented the development of a multi-featured electronic helmet designed to address critical road safety issues. The helmet incorporates advanced functionalities such as GSM and GPS modules, along with systems for detecting overspeeding, accidents, and drunk driving. Besides, the helmet also includes innovative features like solar charging and rain detection. Evaluation and testing confirm the helmet's effectiveness in sending real-time emergency alerts to designated contacts and authorities, facilitated by GSM and GPS for prompt notification and accurate location tracking. Features such as overspeed detection and alcohol level monitoring enhance accountability and safety measures.

The solar charging capability ensures uninterrupted operation of mobile devices, even in remote areas or emergencies, while the rain detection system and internal warming mechanism provide additional comfort and protection, especially in adverse weather conditions. Mandating such helmets with every new vehicle, linked to vehicle documentation, would strengthen compliance with traffic regulations, potentially reducing traffic-related incidents.

Overall, this electronic helmet represents a significant advancement in road safety technology, addressing key challenges such as accident prevention, drunk driving detection, and adverse weather protection. Its mandatory implementation, alongside regulatory measures, could phenomenally improve road safety standards.

Conflicts of Interest

The authors declare no conflict of interest.

References

[1] S. Tapadar, S. Ray, H. N. Saha, A. K. Saha, and R. Karlose, "Accident and Alcohol Detection in Bluetooth Enabled Smart Helmets for Motorbikes," IEEE 8th Annual Computing and Communication Workshop and Conference, pp. 584-590, January 2018.

[2] P. Mishra, P. Pai, P. Singh, V. Kayande, and M. Parmar, "Implementation of a Smart Helmet With Alcohol and Fall Detection and Navigation System," International Conference on Innovative Computing and Communications, vol. 2, pp. 239-251, 2022.

[3] P. Lee, H. Kim, M. S. Zitouni, A. Khandoker, H. F. Jelinek, L. Hadjileontiadis, et al., "Trends in Smart Helmets With Multimodal Sensing for Health and Safety: Scoping Review," JMIR mHealth and uHealth, vol. 10, no. 11, article no. e40797, November 2022.

[4] Y. Chen, Y. Jie, J. Zhu, Q. Lu, Y. Cheng, X. Cao, et al., "Hybridized Triboelectric-Electromagnetic Nanogenerators and Solar Cell for Energy Harvesting and Wireless Power Transmission," Nano Research, vol. 15, no. 3, pp. 2069-2076, March 2022.

[5] X. Zhou, J. Nie, B. Song, Q. Yang, X. Xu, J. Xu, et al., "Ergonomic Evaluation of Thermal Comfort for Different Outlet Distribution Patterns and Ventilation Conditions in the Pilot Protective Helmet," Applied Thermal Engineering, vol. 226, article no. 120355, May 2023.

[6] N. Neha, B. S. Krishnaprasad, and M .L. J. Shruthi, "Real-Time Alcohol Detection and Response System With Arduino and MQ-3 Sensor Integration," 7th International Conference on I-SMAC (IoT in Social, Mobile, Analytics and Cloud), pp. 1095-1103, October 2023.

[7] A. B. Lakshmi, C. Ragunath, R. Yeswanth, and M. Rajkumar, "Smart Helmet for Riders to Avoid Accidents Using IoT," 2nd International Conference on Computer, Communication and Control, pp. 1-4, February 2024.

[8] J. White, C. Thompson, H. Turner, B. Dougherty, and D. C. Schmidt, "Wreckwatch: Automatic Traffic Accident Detection and Notification With Smartphones," Mobile Networks and Applications, vol. 16, no. 3, pp. 285-303, June 2011.

[9] X. Zou, P. Thiruvenkatanathan, and A. A. Seshia, "A Seismic-Grade Resonant MEMS Accelerometer," Journal of Microelectromechanical Systems, vol. 23, no. 4, pp. 768-770, August 2014.

[10] K. Y. Koo, D. Hester, and S. Kim, "Time Synchronization for Wireless Sensors Using Low-Cost GPS Module and Arduino," Frontiers in Built Environment, vol. 4, article no. 82, January 2019.

[11] S. Sharma, K. K. Jain, and A. Sharma, "Solar Cells: In Research and Applications—A Review," Materials Sciences and Applications, vol. 6, no. 12, pp. 1145-1155, December 2015.

[12] C. Udayasri, M. Lavanya, and M Arivalagan, "Solar Based Adjustable Voltage Regulator Using IC LM317," Journal of Chemical and Pharmaceutical Sciences, no. 5, pp. 273-275, October 2016.

[13] J. Ducloux, P. Petrashin, W. Lancioni, and L. Toledo, "Embedded USB Dual-Role System for Communication With Mobile Devices," Argentine School of Micro-Nanoelectronics, Technology and Applications, pp. 1-7, August 2011.

[14] S. Mudi, "Design and Construction of a Portable Solar Mobile Charger," World Academics Journal of Engineering Science, vol. 7, no. 1, pp. 40-44, March 2020.

[15] H. Chowdhury and M. T. Islam, "Multiple Chargers With Adjustable Voltage Using Solar Panel," International Conference on Mechanical Engineering and Renewable Energy, article no. 1-6, November 2015.

[16] C. Iyen, B. Ayomanor, A. Orume, S. Saleh, S. Jaafaru, and B. J. Akeredolu, "Design and Construction of a Rain Detector With an Alarm System," FUW Trends in Science & Technology Journal, vol. 5, no. 3, pp. 686-690, December 2020.

[17] S. Das, S. Mondal, S. Banerjee, and K. Pal, "A Novel Agronomical Technology for Polar Region's Cultivation During Winter Dark," 5th International Conference on Electronics, Materials Engineering & Nano-Technology, pp. 1-6, September 2021.

[18] S. F. Perdana, "AC 220V Digital Thermostat Based Drying Oven XH-W3001 to Improve Temperature Accuracy in the Drying Process of Black Betel Leaves (Piper Betle Var Nigra) at PT. FBION Karanganyar," 2nd International Conference on Early Childhood Education in Multiperspective, vol. 2, pp. 395-406, 2023.

[19] S. Lee, G. Tewolde, and J. Kwon, "Design and Implementation of Vehicle Tracking System Using GPS/GSM/GPRS Technology and Smartphone Application," IEEE World Forum on Internet of Things, pp. 353-358, March 2014.

[20] J. Baramy, P. Singh, A. Jadhav, K. Javir, and S. Tarleka, "Accident Detection & Alerting System," International Journal of Technical Research and Applications, no. 39, pp. 8-11, March 2016.

[21] S. U. Khan, N. Alam, S. U. Jan, and I. S. Koo, "IoT-Enabled Vehicle Speed Monitoring System," Electronics, vol. 11, no. 4, article no. 614, February 2022.

[22] K. Maheswari, U. Madhumitha, S. Madhusurya, and T. Divya, "Alcohol Consumption Detection Using Smart Helmet System," International Journal of Scientific Research in Science, Engineering and Technology, vol. 7, no. 2, pp. 167-173, March-April 2020.

[23] T. Kunatsa, H. C. Myburgh, and A. De Freitas, "Optimal Power Flow Management for a Solar PV-Powered Soldier-Level Pico-Grid," Energies, vol. 17, no. 2, article no. 459, January 2024.

[24] H. A. Attia, B. N. Getu, H. Ghadban, and A. K. A. Mustafa, "Portable Solar Charger with Controlled Charging Current for Mobile Phone Devices," International Journal of Thermal & Environmental Engineering, vol. 7, no. 1, pp. 17-24, 2014.

[25] T. Amosun and W. O. Adedeji, "Design of a PLC Based Temperature Controlled System," REM (Rekayasa Energi Manufaktur) Journal, vol. 8, no. 2, pp. 93-100, December 2023.